Friedrich-Alexander-Universität Erlangen-Nürnberg

Lehrstuhl für Multimediakommunikation und Signalverarbeitung

Prof. Dr.-Ing. André Kaup

Forschungspraktikum

Analyse der Rekonstruktionsqualität eines hybriden Super-Resolution-Ansatzes zur Auflösungserhöhung verrauschter Eingangsdaten

Peter Rudert

August 2016

Betreuer: Dipl. Ing. Michel Bätz

Erklärung

Ich versichere, dass ich die vorliegende Arbeit ohne fremde Hilfe und ohne Benutzung anderer als der angegebenen Quellen angefertigt habe, und dass die Arbeit in gleicher oder ähnlicher Form noch keiner anderen Prüfungsbehörde vorgelegen hat und von dieser als Teil einer Prüfungsleistung angenommen wurde. Alle Ausführungen, die wörtlich oder sinngemäß übernommen wurden, sind als solche gekennzeichnet.

_____ _____

Ort, Datum Unterschrift

Contents

Chapter 1

Introduction

In the field of video surveillance, low cost sensors are often used. The reason is to reduce the data storage or to improve the cost efficiency. Consequently, the quality is reduced and thus details like a number plate or a face can not be perceived any more. For entertainment systems, it is also a problem to display a high-quality video sequence even though a low resolution (LR) video is given.

Therefore, Bätz et al. in [1] introduce a super resolution (SR) algorithm to erase this problem. The idea of this approach is to combine two approaches into one: single-image SR (SISR) and multi-image SR (MISR) combined to hybrid super-resolution (HYSR). SISR takes one picture into account whereas MISR uses multiple frames of a video sequence. SISR is less computationally expensive and does not generate any errors made by the motion estimation. But on the other hand it does not restore as many details as MISR. Having multiple images has the benefit to improve the quality of the output. HYSR makes soft decisions whether SISR or MISR is to compute on specific parts of the picture. For static video sequences the SISR method is used and for moving parts MISR is utilized. The final goal of this approach is to improve the PSNR value and to get a better visual quality.

This report is subdivided into three chapters. The first one is the introduction. In Chapter 2 of this report, the theoretical backgrounds of SISR, MISR, and HYSR are introduced. The third chapter is divided into three parts. At first, the simulation results from Bätz et al. [1] are shown. Bätz et al. [1] simulated the HYSR approach without adding noise on the pictures. Secondly this report presents the result of the simulation of adding noise to the low resolution pictures. Thirdly, it depicts the effect of canceling the artificial-made noise by processing it in various ways. In the last chapter, a conclusion is drawn.

Chapter 2

Theoretical Background

2.1 Single-Image Super-Resolution

The Single-Image SR (SISR) approach applied in this report was presented by Kim et al. [3] and uses an example-based learning approach. For further information, it is referred to Bätz et al. [1] and Kim et al. [3], who describe the realization and the theory of this approach, respectively.

2.2 Multi-Image Super-Resolution

The idea of multi-image SR (MISR) is to take several neighbor images and exploit the correlation between the same areas over various pictures. To explain the single steps of the algorithm, it is useful to look at the observation model from a mathematical point of view:

$$\mathbf{I}_{LR,k} = \mathbf{DBM}_k\mathbf{I}_{HR} + n_k, \text{ for } 1 \leq k \leq M, \tag{2.1}$$

where $\mathbf{D}$, $\mathbf{B}$, and $\mathbf{M}_k$ stand for downsampling, blurring and motion to each neighboring frame, respectively. n_k is a noise vector, M is the amount of LR frames and $\mathbf{I}_{HR}$ depicts the high resolution frame. In general, there are three steps to restore the desired HR

image $\mathbf{I}_{HR}$ from $\mathbf{I}_{LR,k}$. Step one is applying an optical flow approach onto the current frame. The next step is to interpolate these non-uniformly distributed points onto the HR image grid. At last the super-resolved image is obtained in the restoration step. That is done by the Lucy-Richardson deconvolution in all simulations in Chapter 3 except for Section 3.3.2, which takes a Wiener filter algorithm instead.

2.3 Hybrid Super-Resolution

The hybrid super-resolution (HYSR) approach gets as input a low resolution image $I_{LR}[\tilde{m}, \tilde{n}, t]$, where $(\tilde{m}, \tilde{n})$ denotes the LR coordinates and t depicts the current frame. Firstly, the algorithm is split up into one part computing the SISR result $\mathbf{I}_{SISR}[m, n, \tau]$ and the other part computes the MISR image $\mathbf{I}_{MISR}[m, n, \tau]$. SISR and MISR use the approaches described in Sections 2.1 and 2.2, respectively. MISR takes $\frac{N-1}{2}$ frames each before and after the current frame t into account.

A reliable decision is made by a soft decision mask $\mathbf{H}[m, n]$. This matrix decides for which area in the picture which mode is applied. The value of this matrix is proportional to the availability of consistent motion vectors over all N images.

If there was no motion or wrong motion estimation, values will get to zero and SISR is applied. On the other hand MISR has more impact on the output for higher values of $\mathbf{H}[m, n]$. Bätz et al. [1] reveals more information about the derivation of this parameter.

Chapter 3

Practical Part

All simulations presented in this paper use the hybrid super-resolution approach. 'BQMall', 'panslow', 'spincalender', 'BQTerrace', 'Kimono1' and 'Traffic' are the applied video sequences and have a spatial resolution of 832 × 480, 1280 × 720, 1280 × 720, 1920 × 1080, 1920 × 1080, 2560 × 1600, respectively. The upscaling factor for all simulations is 4. The simulations without noise in Section 3.1 and the simulations with noise in Section 3.2 were simulated with all six video sequences as input.

However, for the preprocessing simulation in Section 3.3.1 only 'BQMall' was taken into account. The post-processing part in the same section uses 'BQMall', 'panslow', 'spincalender' and 'BQTerrace' as input.

For testing the performance of the Wiener filter in Section 3.3.2 three video sequences 'BQMall', 'panslow' and 'spincalender' were used. Thus, the simulation results in Section 3.3 cannot be compared entirely to the results from Section 3.1 and 3.2. But they point out a trend that might be achieved using these countermeasures.

All other parameters, which are needed for the HYSR algorithm, are described by Bätz et al. [1].

In Section 3.2 and 3.3 each pixel of the video sequences was degraded by a zero-mean Gaussian noise. There are three different values for the noise variance σ^2 to see

how HYSR and the countermeasures react to various kinds of distortion. The values $\sigma_1^2 = 0.00005$, $\sigma_2^2 = 0.0007$ and $\sigma_3^2 = 0.0025$ were chosen. They were given into the MATLAB function *imnoise*, which adds Gaussian noise onto one image which has only values between 0 and 1. Thus, the SNR of the images is not constant because an absolute noise power was added which is independet of the picture's variance.

The quality criteria in this report is the PSNR gain relatively to bicubic interpolation over the number of utilized frames N.

3.1 Simulation Results Without Noise

The result of the simulation without noise is depicted in Fig. 3.1. It shows the average PSNR value over all 30 frames and six sequences for SISR, MISR and HYSR over a different number of utilized frames. It can be seen that all three approaches have a higher value than bicubic interpolation. The green dot stands for SISR and has a gain of 0.25 dB. MISR has a maximimum gain of 1.10 dB in case of seven utilized frames. Being better than MISR and SISR at every number of utilized frame shows the superiority of HYSR. However, at $N = 3$ its PSNR gain is close to MISR because SISR has a negative impact on the output. HYSR has its maximum at $N = 9$ where it has a gain of 1.48 dB. Apart from this objective enhancement there is also achieved an visual improvement which is described by Bätz et al. [1].

3.2 Simulation Results With Noise

Fig. 3.2 depicts the effect of different noise variances on the PSNR gain of the three super-resolution approaches.
In case of σ_1^2 in Fig. 3.2 (a) the same behaviour as the simulation without noise in Section 3.1 can be seen, apart from small offsets for each approach. SISR and MISR at the point $N = 5$ have a maximum gain of 0.15 dB and 0.91 dB, respectively. HYSR

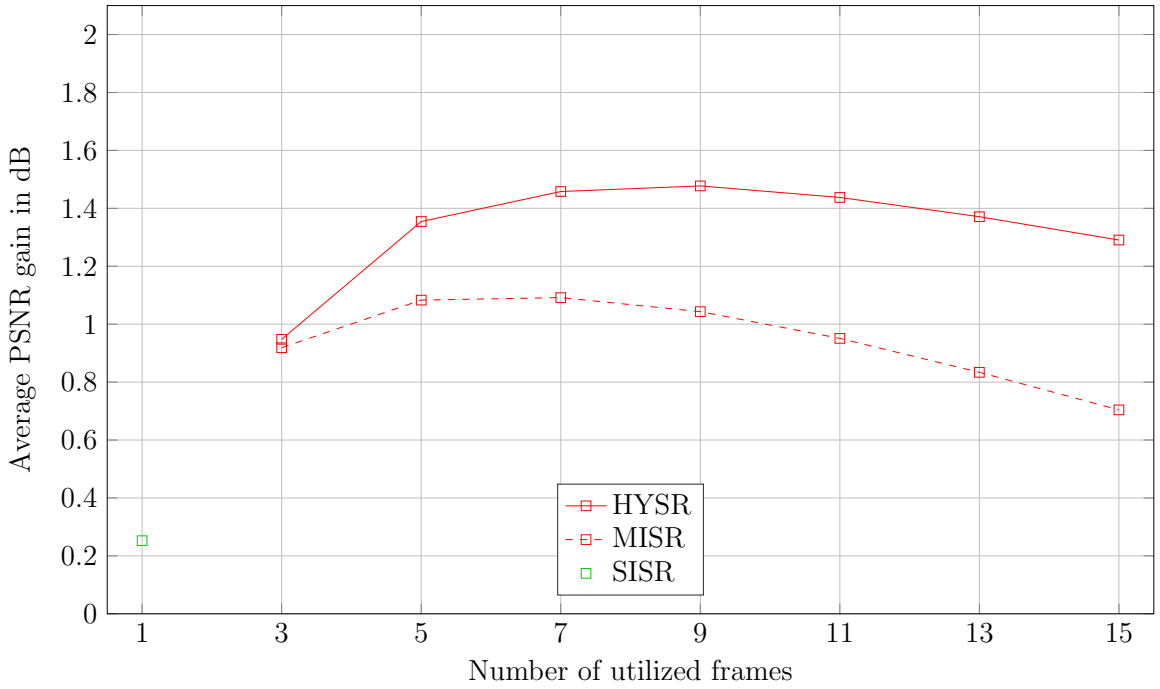

Figure 3.1: Average PSNR gain (in dB) over bicubic interpolation over the number of utilized frames N.

is still the best approach with the highest value 1.35 dB at $N = 9$.

σ_2^2 changes the behavior of the curves in Fig. 3.2 (b) and the offset is even bigger for all algorithms. SISR has a gain of -1.02 dB and MISR gets a maximum gain of -0.39 dB for $N = 5$. Therefore, both approaches are worse off than bicubic interpolation in this case. HYSR is better than bicubic interpolation for frames greater than $N = 3$ with a maximum of 0.39 dB at $N = 7$.

The last test case holds the strongest noise distortion σ_3^2 displayed in Fig.3.2 (c). The PSNR gain of SISR goes down to -1.87 dB and the maximum gain of MISR gets up to -1.51 dB at $N = 3$. HYSR is no longer better than bicubic interpolation at any point. Its highest value is -0.47 dB at $N = 5$.

To get a better visual impression about the distortion generated by the Gaussian noise Fig. 3.3 (b) to 3.3 (d) shows the same image of scenario 'BQMall' for the three different noise variances. Frame number was set to 218 arbitrarily and all pictures

have LR quality. Fig. 3.3 (a) depicts the reference picture without noise.
The image in Fig. 3.3 (b) displays the effect of σ_1^2 on the picture. The outcome is hardly visible, only on homogenous regions is a certain distortion in form of uneveness visible.
Fig 3.3 (c) and 3.3 (d) have a Gaussian noise distortion with the variances σ_2^2 and σ_3^2, respectively. Both images have a higher perceivable degradation of the image quality. Fig 3.3 (d) is the most distorted and, hence, has lost the most details, for instance the contour of a face.

3.3 Countermeasures

Two countermeasures are now proposed to reduce the effect of noise on the images. One is the CBM3D algorithm published by Dabov et al. [2]. It is used for the simulation results presented in Section 3.3.1.
With the help of this approach a pre-processing and a post-processing based simulation was run. Processing means in that case that the noise was suppressed by a Matlab algorithm. Pre-processing was applied just after noise was added to the image. Post-processing inherits the same algorithm but it is performed before the restoration step. The other countermeasure is a Wiener filter algorithm. The simulation results for this second processing step can be found in Section 3.3.2.

3.3.1 CBM3D

Fig. 3.4 displays the average PSNR gain for the three noise variances for the case pre-processing.
Using σ_1^2 the PSNR results are improved in comparison to the noisy values from Fig. 3.2 (a). HYSR has still the best gains except for $N = 3$ where MISR is slightly better. The PSNR gains of MISR and HYSR decrease when using a variance of σ_2^2 illustrated in Fig. 3.4 (c). However, the value for SISR increases.
The last simulation results, displayed in Fig. 3.4 (c), are all lower than the previous

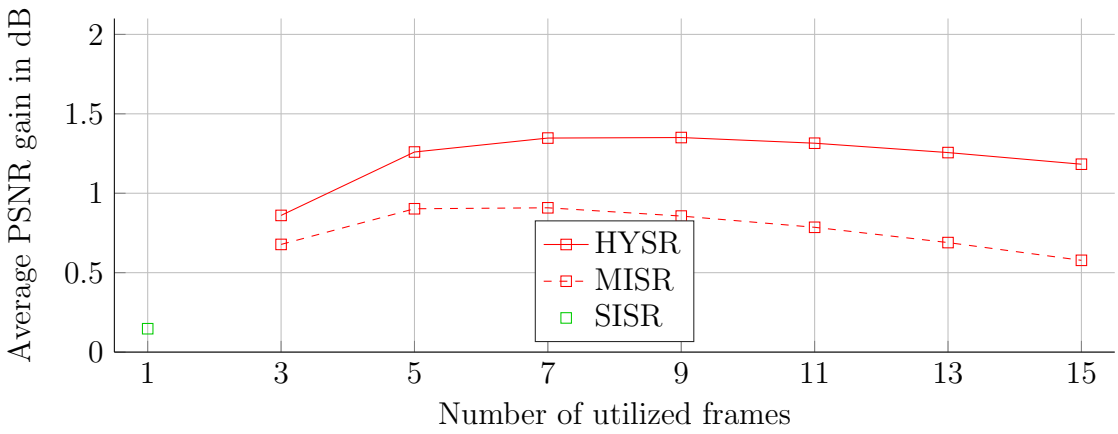

(a)

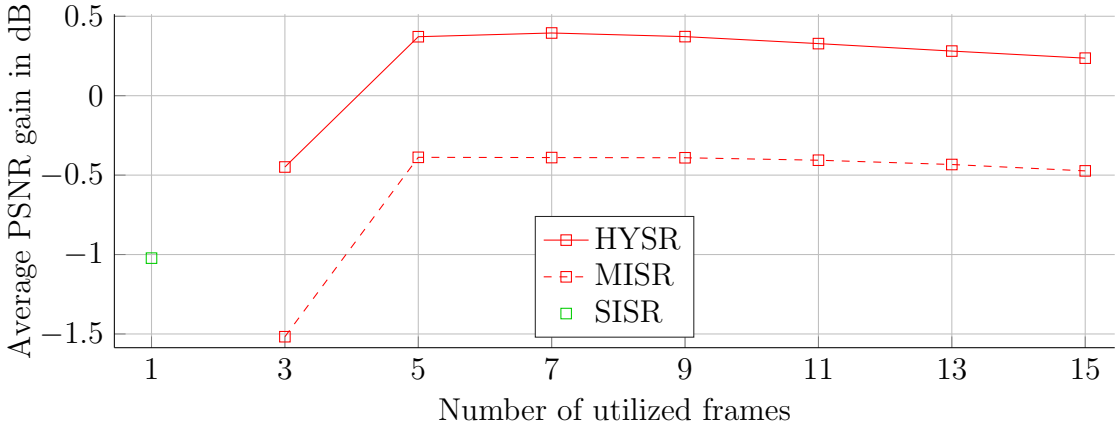

(b)

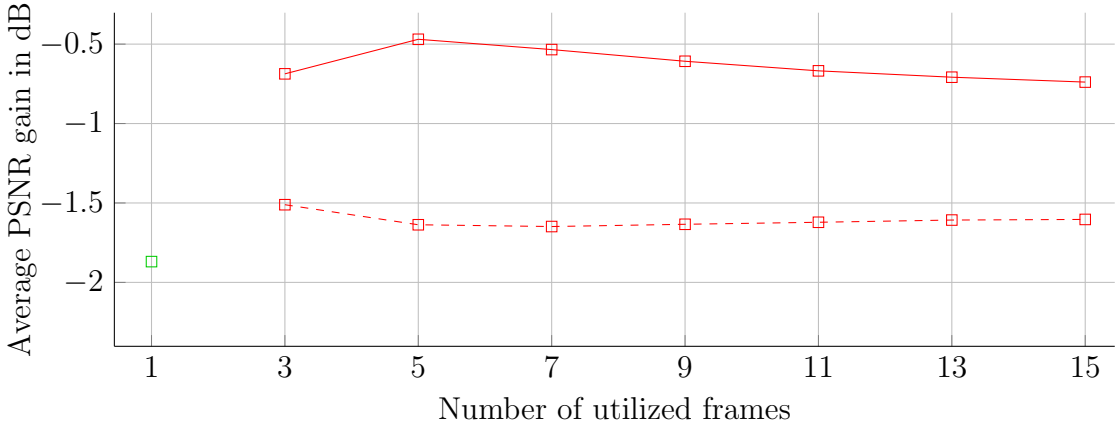

(c)

Figure 3.2: Average PSNR gain (in dB) over bicubic interpolation over the number of utilized frames N. The simulation was run with the noise variances σ_1^2 in (a), σ_2^2 in (b) and σ_3^2 in (c), respectively.

(a) (b)

(c) (d)

Figure 3.3: Visual quality comparison of the various variance level for the example scenario 'BQMall'. Frame number 218 is used for noise variances σ_1^2 in (b), σ_2^2 in (c) and σ_3^2 in (d), respectively. (a) is the reference LR image before adding noise.

ones. Still HYSR holds the best performance and all approaches are still better than bicubic interpolation for all N.

Post-processing shows an improvement of the PSNR values in Fig. 3.5 for all super-resolution approaches over all noise variances in comparison to the correspondent results shown in Section 3.2.

Moreover, post-processing is better than pre-processing at any number of utilized frame for any variance.

However, there are some oddities that are revealed in Fig. 3.5. Firstly, SISR has a too low gain of -1.51 dB for a noise variance σ_3^2 so that it can not displayed in 3.5 (c) anymore. Besides, the gains in Fig. 3.5 (c) of MISR and HYSR for σ_3^2 are higher

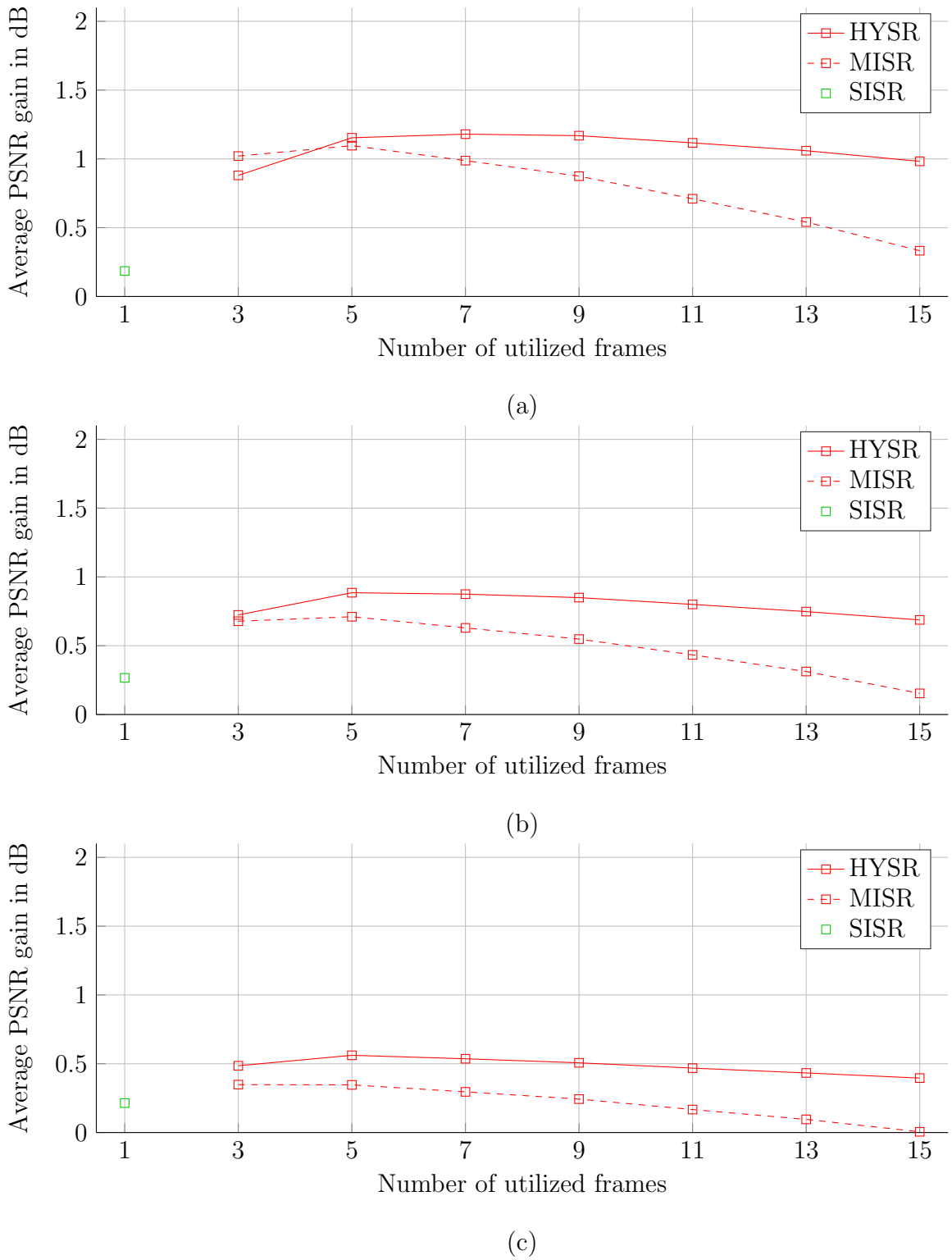

Figure 3.4: Average PSNR gain (in dB) over bicubic interpolation over the number of utilized frames N. Applied is the denoise algorithm CBM3D in pre-processing mode for noise variances σ_1^2 in (a), σ_2^2 in (b) and σ_3^2 in (c), respectively.

than the values in Fig. 3.5 (b). Expected was the opposite because σ_3^2 leads to bigger distortion than σ_2^2. Thus, it ought to lead to more loss of signal power and to a smaller PSNR.

Another unanticipated point is that MISR has higher values than HYSR in Fig. 3.5 (c) what is not expected neither. The reason for this might be that HYSR is dependent of the quality of SISR and MISR. If now the PSNR of SISR is now clearly worse than the one of MISR the result of MISR gets worse than the PSNR of MISR.

3.3.2 Wiener Filter

To review the influence of the Lucy-Richardson deconvolution on the HYSR approach a Wiener filter was used in this simulation. Its task is to remove the noise and to deblur the picture simultaneously.

The effect of this tool on the PSNR is pretty humble, however. Fig. 3.6 shows that MISR and HYSR are always worse off for all noise variances compared to the cases of no processing. Only SISR achieves a higher gain for the variances σ_2^2 and σ_3^2 seen in Fig. 3.6 (b) and 3.6 (c).

The reason for that big loss of gain might be that the Wiener filter creates undesireable artifacts. Decreasing PNSR gain with increasing number of utilized frames for MISR and HYSR supports this theory.

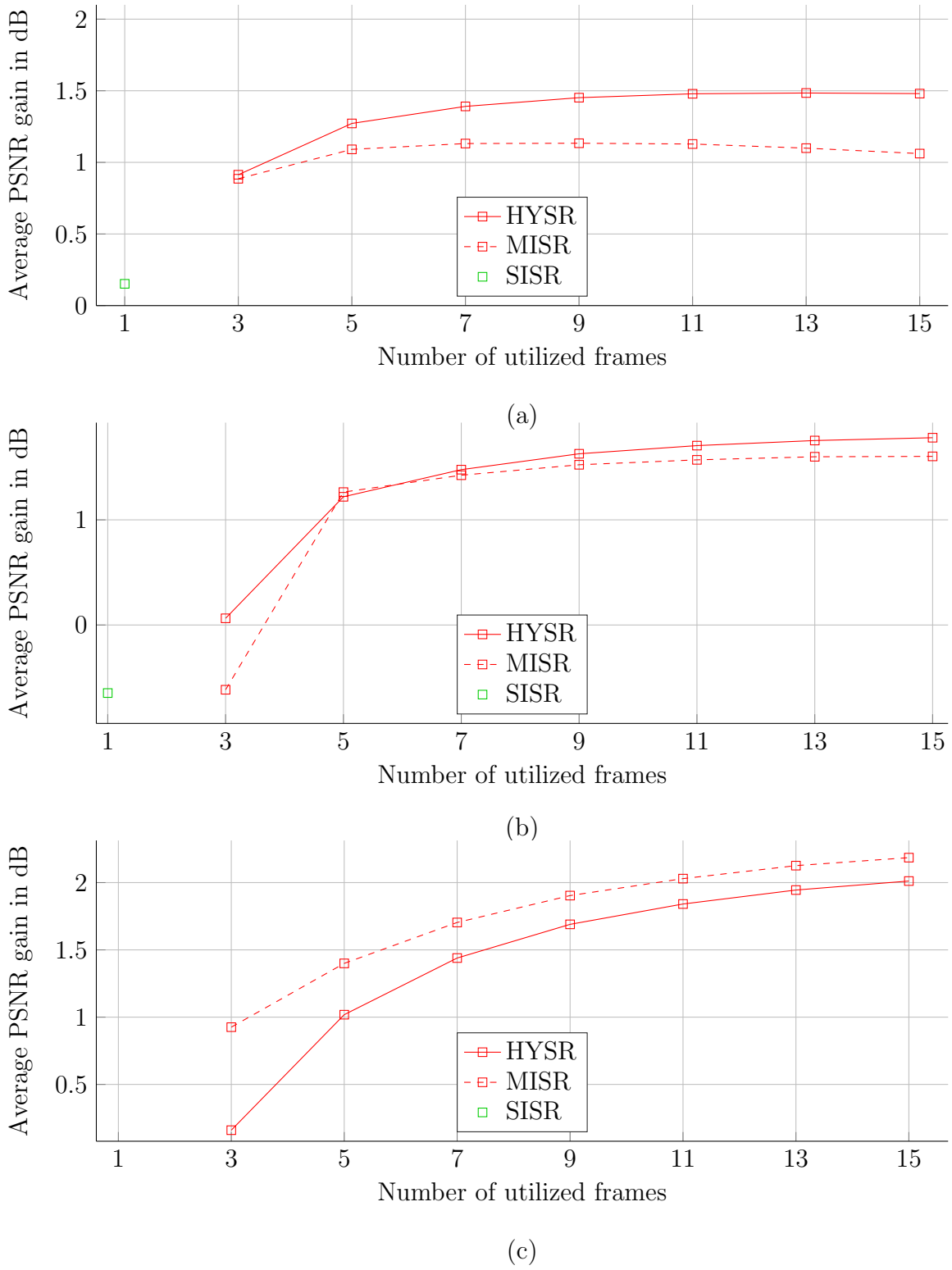

Figure 3.5: Average PSNR gain (in dB) over bicubic interpolation over the number of utilized frames N. Applied is the denoise algorithm CBM3D in post-processing mode for noise variances σ_1^2 in (a), σ_2^2 in (b) and σ_3^2 in (c), respectively.

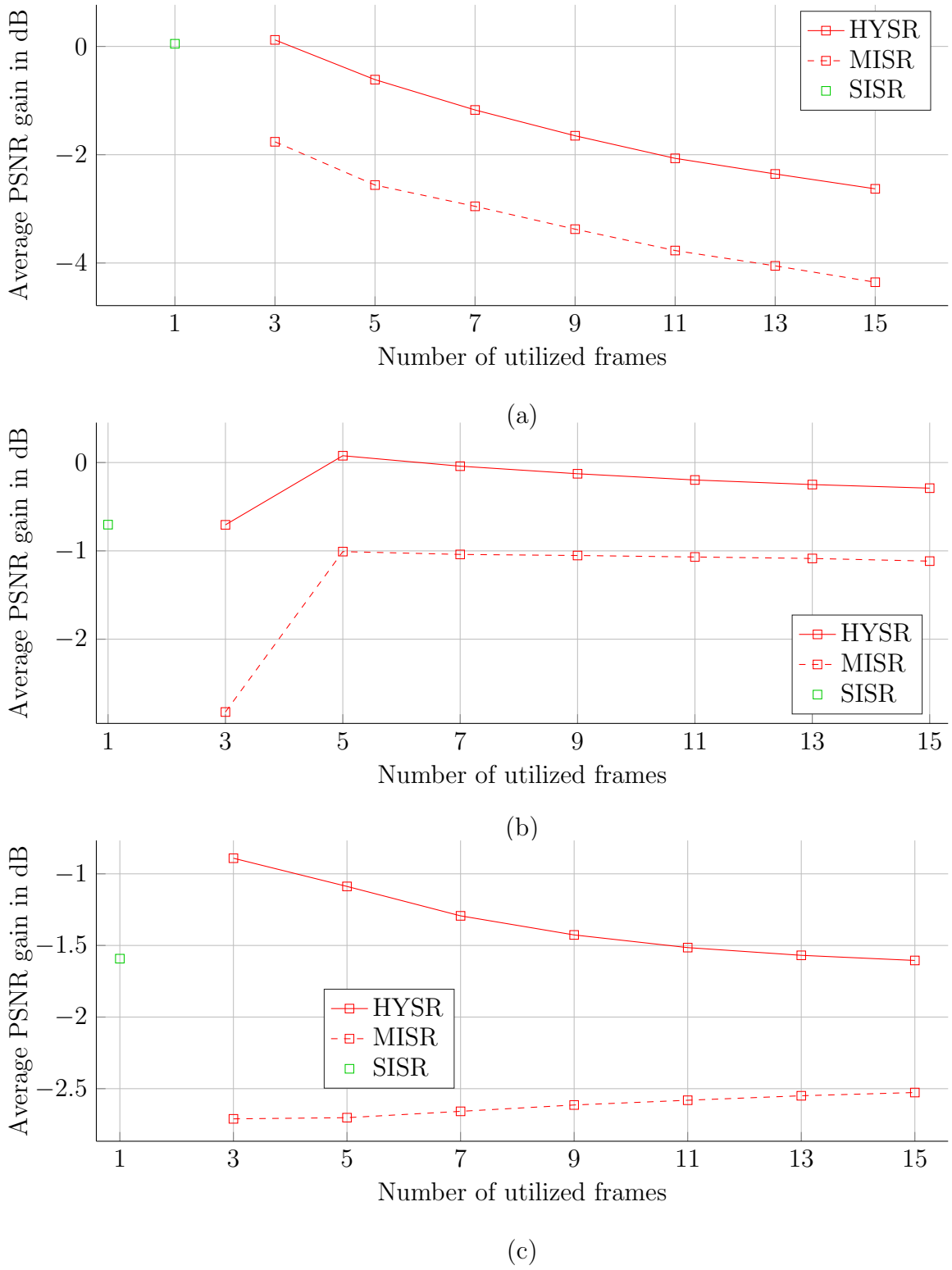

Figure 3.6: Average PSNR gain (in dB) over bicubic interpolation over the number of utilized frames N. Applied is a Wiener filter for noise variances σ_1^2 in (a), σ_2^2 in (b) and σ_3^2 in (c), respectively

Chapter 4

Conclusion

This report dealt with the introduction of the new approach HYSR at first. HYSR is a novel combination of single-image and multi-image super-resolution. The outcome was to get a a resolution enhancement compared to SISR, MISR and bicubic interpolation. To investigate the effect of noisy images as input on the HYSR performance three simulation results with each three different noise variances were presented then. The result showed that the PSNR gain of HYSR over bicubic interpolation decreases with increasing noise variance. However, HYSR was always better than SISR and MISR. Additionally, for two out of three simulations it had a positive gain over bicubic interpolation.

Afterwards, two processing algorithms were proposed to reduce the effect of noisy images. One was the so-called CBM3D and the other one was a Wiener filter. CBM3D was placed at two different places in the HYSR approach, therefore it was called pre- and post-processing, respectively. Both processing tools made an improvement in comparison to the simulation results with noise. However, doing a post-processing achieved an even higher gain compared to pre-processing.
The Wiener filter did not improve the quality, it rather amplified the distortion. Consequently, the simulation results were even worse than the results with noise.

Overall, this chapter showed that the best processing tool against noise is the CBM3D algorithm placed just before the deconvolution step.

Appendix A

Tables

	utilized frames N	Bicubic	SISR	MISR	HYSR
$\sigma^2 = 0$	3	26.74	26.88	27.82	27.63
	5	26.74	26.88	27.90	27.92
	7	26.74	26.88	27.79	27.97
	9	26.74	26.88	27.68	27.97
	11	26.74	26.88	27.50	27.91
	13	26.74	26.88	27.33	27.86
	15	26.74	26.88	27.10	27.77
	Average gain over bicubic	-	0.14	0.85	1.12

Table A.1: Average PSNR results (in dB) over the number of utilized frames N for the scenario 'BQMall'.

	utilized frames N	Bicubic	SISR	MISR	HYSR
σ_1^2	3	26.67	26.75	27.29	27.44
	5	26.67	26.75	27.70	27.80
	7	26.67	26.75	27.58	27.82
	9	26.67	26.75	27.46	27.81
	11	26.67	26.75	27.30	27.75
	13	26.67	26.75	27.13	27.69
	15	26.67	26.75	26.91	27.61
	Average gain over bicubic	-	0.08	0.67	1.03
σ_2^2	3	25.88	25.07	25.78	26.07
	5	25.88	25.07	25.75	26.38
	7	25.88	25.07	25.68	26.34
	9	25.88	25.07	25.61	26.29
	11	25.88	25.07	25.51	26.22
	13	25.88	25.07	25.40	26.15
	15	25.88	25.07	25.25	26.08
	Average gain over bicubic	-	-0.80	-0.31	0.34
σ_3^2	3	24.22	22.48	22.94	23.54
	5	24.22	22.48	22.78	23.76
	7	24.22	22.48	22.70	23.68
	9	24.22	22.48	22.66	23.61
	11	24.22	22.48	22.62	23.55
	13	24.22	22.48	22.57	23.50
	15	24.22	22.48	22.51	23.46
	Average gain over bicubic	-	-1.74	-1.54	-0.64

Table A.2: Average PSNR results (in dB) over the number of utilized frames N for the scenario 'BQMall'. The simulation was run with the noise variances σ_1^2, σ_2^2, and σ_3^2, respectively.

		Pre processing				Post processing			
	utilized frames N	Bicubic	SISR	MISR	HYSR	Bicubic	SISR	MISR	HYSR
σ_1^2	3	26.65	26.84	27.67	27.53	26.67	26.75	27.73	27.51
	5	26.65	26.84	27.75	27.80	26.67	26.75	27.85	27.84
	7	26.65	26.84	27.64	27.83	26.67	26.75	27.75	27.89
	9	26.65	26.84	27.52	27.82	26.67	26.75	27.64	27.90
	11	26.65	26.84	27.36	27.77	26.67	26.75	27.49	27.85
	13	26.65	26.84	27.19	27.71	26.67	26.75	27.33	27.80
	15	26.65	26.84	26.98	27.63	26.67	26.75	27.11	27.73
	Average gain over bicubic	-	0.18	0.79	1.08	-	0.08	0.89	1.12
		Bicubic	SISR	MISR	HYSR	Bicubic	SISR	MISR	HYSR
σ_2^2	3	26.02	26.29	26.70	26.74	25.88	25.07	26.83	26.35
	5	26.02	26.29	26.73	26.90	25.88	25.07	27.08	26.95
	7	26.02	26.29	26.65	26.89	25.88	25.07	27.13	27.13
	9	26.02	26.29	26.57	26.87	25.88	25.07	27.13	27.21
	11	26.02	26.29	26.45	26.82	25.88	25.07	27.09	27.22
	13	26.02	26.29	26.33	26.77	25.88	25.07	27.02	27.21
	15	26.02	26.29	26.17	26.71	25.88	25.07	26.89	27.17
	Average gain over bicubic	-	0.27	0.50	0.80	-	-0.80	1.15	1.16
		Bicubic	SISR	MISR	HYSR	Bicubic	SISR	MISR	HYSR
σ_3^2	3	25.11	25.33	25.46	25.60	24.22	22.48	25.15	24.19
	5	25.11	25.33	25.46	25.67	24.22	22.48	25.58	25.02
	7	25.11	25.33	25.41	25.65	24.22	22.48	25.80	25.34
	9	25.11	25.33	25.35	25.62	24.22	22.48	25.93	25.52
	11	25.11	25.33	25.28	25.58	24.22	22.48	25.99	25.61
	13	25.11	25.33	25.21	25.54	24.22	22.48	26.02	25.66
	15	25.11	25.33	25.12	25.51	24.22	22.48	26.01	25.68
	Average gain over bicubic	-	0.21	0.21	0.48	-	-1.74	1.56	1.06

Table A.3: Average PSNR results (in dB) over the number of utilized frames N for the scenario 'BQMall'. Applied is the denoise algorithm CBM3D in pre- and post-processing mode for noise variances σ_1^2, σ_2^2, and σ_3^2, respectively.

	utilized frames N	Bicubic	SISR	MISR	HYSR
σ_1^2	3	26.67	26.75	25.03	26.85
	5	26.67	26.75	24.25	26.15
	7	26.67	26.75	23.62	25.50
	9	26.67	26.75	23.07	24.97
	11	26.67	26.75	22.58	24.53
	13	26.67	26.75	22.08	24.15
	15	26.67	26.75	21.56	23.80
	Average gain over bicubic	-	0.08	-3.50	-1.53
	utilized frames N	Bicubic	SISR	MISR	HYSR
σ_2^2	3	25.88	25.07	24.94	25.86
	5	25.88	25.07	24.84	25.93
	7	25.88	25.07	24.74	25.77
	9	25.88	25.07	24.66	25.64
	11	25.88	25.07	24.56	25.53
	13	25.88	25.07	24.45	25.45
	15	25.88	25.07	24.30	25.36
	Average gain over bicubic	-	-0.80	-1.23	-0.23
	utilized frames N	Bicubic	SISR	MISR	HYSR
σ_3^2	3	24.22	22.48	21.49	23.19
	5	24.22	22.48	21.50	23.09
	7	24.22	22.48	21.52	22.90
	9	24.22	22.48	21.54	22.77
	11	24.22	22.48	21.55	22.69
	13	24.22	22.48	21.55	22.64
	15	24.22	22.48	21.55	22.61
	Average gain over bicubic	-	-1.74	-2.70	-1.38

Table A.4: Average PSNR results (in dB) over the number of utilized frames N for the scenario 'BQMall'. Applied is a Wiener filter for noise variances σ_1^2, σ_2^2, and σ_3^2, respectively.

Bibliography

[1] M. Bätz, A. Eichenseer, J. Seiler, M. Jonscher, and A. Kaup. Hybrid super-resolution combining example-based single-image and interpolation-based multi-image reconstruction approaches. In *Image Processing (ICIP), 2015 IEEE International Conference on*, pages 58–62, Sept 2015.

[2] K. Dabov, A. Foi, V. Katkovnik, and K. Egiazarian. Image denoising by sparse 3-d transform-domain collaborative filtering. *IEEE Transactions on Image Processing*, 16(8):2080–2095, Aug 2007.

[3] K. I. Kim and Y. Kwon. Single-image super-resolution using sparse regression and natural image prior. *IEEE Transactions on Pattern Analysis and Machine Intelligence*, 32(6):1127–1133, June 2010.